I-EDU GROUP

MSU

Article

Parity-Dependent Pancreatic Morphological and Morphometric Changes in Intrahepatic Cholestasis of Pregnancy: An Autopsy Study

Bobir Khoshimov [1], **Sherzod Kenjayev** *[2]

[1] Department of Clinical Sciences, Alfraganus University, Tashkent, 100190, Uzbekistan
[2] Department of Traumatology and Orthopedics, Fergana Medical Institute of Public Health, Fergana, 150100, Uzbekistan
usmleu6@gmail.com (B.Kh.), sherzodbek.4512@gmail.com (S.K.)
* Correspondence: sherzodbek.4512@gmail.com; Tel.: +998 95 640 43 93

Abstract:

Aim. To characterise the morphological and morphometric changes of the pancreas, and their relationship with hepatic injury and pregnancy parity, in women who died with intrahepatic cholestasis of pregnancy (ICP).

Materials and Methods. An autopsy-based morphological and quantitative morphometric study was performed on liver and pancreatic tissue from 51 women who died with severe ICP (Republican Scientific and Practical Center of Pathological Anatomy, 2013–2023), compared with 12 fertile-age controls who died of acute myocardial infarction. Sections were stained with haematoxylin–eosin and digitised for morphometry (12 parameters) in 28 index cases and controls; means were compared using Student's t-test.

Results. ICP livers showed centrilobular and midzonal hepatocellular cholestasis, bile-pigment accumulation, hydropic dystrophy and necrobiosis (54.2%), with canalicular bile stasis in 75% of cases. The pancreas showed bile reflux into major and lobular ducts, segmental acinar necrosis, vacuolar dystrophy, interstitial oedema, periductal infiltration and progressive fibrosis. All 12 morphometric indices differed significantly from controls ($P < 0.01$–$P < 0.001$), and severity increased with parity, being most pronounced in the third and fourth pregnancies.

Conclusion. ICP is a systemic, bile-acid-mediated toxic condition producing quantifiable, parity-dependent pancreatic injury alongside hepatic cholestasis, supporting closer pancreatic surveillance in severe or recurrent ICP.

Keyword: intrahepatic cholestasis of pregnancy, pancreas, liver, morphometry, parity, bile acids, autopsy, pancreatitis, islets of Langerhans, histopathology.

Quoting: Bobir Khoshimov, Sherzod Kenjayev. Parity-Dependent Pancreatic Morphological and Morphometric Changes in Intrahepatic Cholestasis of Pregnancy: An Autopsy Study. **2026**, 5, 2, 6. https://doi.org/10.56121/MSU-2026-2-00012

Received: 27.02.2026
Corrected: 18.03.2026
Accepted: 20.03.2026
Published: 30.04.2026

Introduction

Intrahepatic cholestasis of pregnancy (ICP) is the most common pregnancy-specific liver disorder, typically presenting with pruritus and elevated serum bile acids in the second or third trimester [1]. Its estimated incidence lies between 1.5% and 2% of all pregnancies worldwide — translating into roughly 4.5–9.0 million affected women each year — with even higher regional prevalence reported in several countries of Central Asia and the Commonwealth of Independent States [1,2]. Although maternal prognosis is generally favourable, ICP is far from a benign biochemical curiosity: a two-fold rise in serum bile acid concentration has been associated with a substantially increased risk of stillbirth and of spontaneous or iatrogenic preterm birth, particularly once bile acid concentrations exceed 40–100 μmol/L [3,4].

The pathogenesis of ICP centres on impaired canalicular bile acid transport under the influence of elevated oestrogen and progesterone metabolites, leading to intracellular and systemic bile acid accumulation [1,5]. Because bile acids are potent detergents and signalling molecules, their supra-physiological retention is increasingly recognised as a systemic, rather than purely hepatobiliary, insult: bile acid receptor pathways such as the farnesoid X receptor (FXR) and TGR5 govern not only

hepatocellular and cholangiocyte homeostasis but also epithelial–mesenchymal transition, fibrogenesis and apoptosis in bile-exposed tissue throughout the digestive system [6–8]. Experimental models of ICP have further demonstrated bile-acid-induced mitochondrial dysfunction and disruption of the Bcl-2/Bax apoptotic balance in placental trophoblasts [9,10], and a recent genome-wide association meta-analysis of more than 440,000 women identified genetic loci shared between ICP and acute pancreatitis, providing the first population-scale evidence that the two conditions may share pathogenic mechanisms [11]. Consistent with this, isolated case reports have described clinically overt pancreatitis complicating or preceding severe ICP [12,13], yet a systematic pathomorphological characterisation of the pancreas in fatal ICP has not, to our knowledge, previously been undertaken.

Given that the exocrine pancreas drains via a duct system anatomically and functionally continuous with the extrahepatic biliary tree, and that bile acids reaching supraphysiological concentrations are directly cytotoxic to ductal and acinar epithelium [6,14], it is biologically plausible that the pancreas is a "silent" target organ in ICP whose injury is overshadowed clinically by hepatic and obstetric manifestations. Whether such injury accumulates with successive pregnancies — a question of particular relevance in populations with high parity — has not previously been addressed, even though parity is already known to modify the natural history of ICP itself [15,16], and novel biomarkers of cholestatic severity, such as Xenin-25, correlate with hepatic stress and fibrosis indices [17].

This study therefore aimed to characterise, by autopsy-based light microscopy and quantitative digital morphometry, the morphological changes of the pancreas — set against the corresponding hepatic findings — in women who died with severe ICP, and to determine whether the severity of pancreatic injury is related to pregnancy parity.

Materials and Methods

Study design and ethics

This retrospective, autopsy-based morphological, histochemical and morphometric study was approved by the Scientific Committee of the Fergana Medical Institute of Public Health (FMIOPH), minutes dated 25 September 2025. All autopsy material was archival and anonymised, obtained during routine forensic-pathological examination performed independently of this study. Because the study used retrospective, de-identified archival tissue rather than data or specimens obtained from living participants, individual informed consent was waived by the Ethics Committee, consistent with national regulations governing the use of archival pathological material.

Study population

Liver and pancreatic tissue was retrieved from the archive of the Republican Scientific and Practical Center of Pathological Anatomy for the period 2013–2023. The main group comprised 51 women of fertile age who died with clinically and biochemically confirmed severe ICP; the control group comprised 12 fertile-age women, of comparable age, who died of acute myocardial infarction and had no antemortem or autopsy evidence of hepatobiliary or pancreatic disease. The combined series (n=51) was stratified by pregnancy parity at the time of death (first, third, fourth and fifth pregnancy: 7, 41, 11 and 4 cases, respectively) to evaluate a possible parity–severity relationship.

Tissue processing and light microscopy

Standard autopsy samples of liver and pancreas (head, body and tail) were fixed in 10% neutral buffered formalin, routinely processed, embedded in paraffin, sectioned at 4–5 μm and stained with haematoxylin and eosin (H&E). Sections were examined by light microscopy at magnifications ranging from $\times$40 to $\times$400.

Digital morphometry

For quantitative analysis, 28 index cases were selected from the 51 ICP cases; glass slides from these 28 cases and all 12 controls were digitised using a NanoZoomer whole-slide scanner, consistent with contemporary approaches to computer-assisted, reproducible histomorphometric assessment [18,19]. Two-dimensional tangential sections were analysed using three standardised fields of view — 32,000 μm^2, 64,000 μm^2 and 128,000 μm^2 — along the X and Y axes. For each case, 8–10 microsamples were prepared, and the arithmetic mean for each field size was calculated; case-level means were then averaged across the study and control groups. Twelve parameters were measured: mean acinocyte nuclear diameter; acinar cell cytoplasmic area; mean cross-sectional area

of the islets of Langerhans; thickness of the pancreatic interstitium; mean diameter of capillaries and venules; proportion of acinocytes showing vacuolar/granular dystrophy; number of apoptotic/necrotic cells per field; periductal inflammatory infiltration density; number of diapedetic haemorrhagic foci; proportion of the section occupied by connective tissue; desquamation index of the ductal epithelium; and a composite microvascular congestion index.

Statistical analysis

The relationship between pregnancy parity and pancreatic morphometric severity within the ICP group was assessed using Spearman's rank correlation coefficient (ρ) between parity number and each morphometric index; a two-tailed P value < 0.05 was considered statistically significant.

Results

Hepatic morphological changes

In ICP cases, hepatocytes of the centrilobular zone (zone 3) showed variable-sized, coarse, golden-brown to dark-brown intracytoplasmic bile-pigment granules, associated with necrosis of individual hepatocytes and dense aggregates of pigment-laden macrophages (Figure 1). Bile-pigment accumulation was not confined to zone 3: hepatocytes of the intermediate, midzonal region (zone 2) also displayed diffuse, finely granular cytoplasmic bile pigment, with expansion and vacuolisation of the cytoplasm and progression to hydropic degeneration in the more severely affected cells (Figure 2). Overall, bile stasis was identifiable within canaliculi and ductules in 75% of cases, and hepatocellular necrobiosis was present in 54.2% of cases, most often accompanied by mixed macrophage–lymphocytic portal and lobular infiltration.

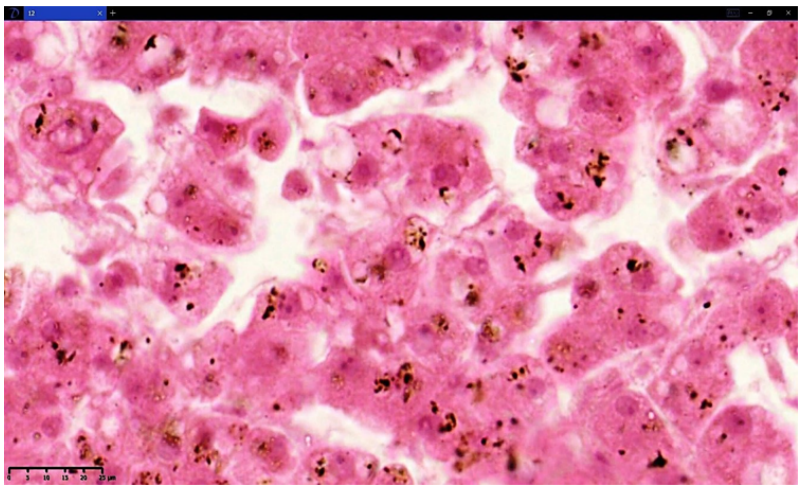

Figure 1. Liver, intrahepatic cholestasis of pregnancy. Centrilobular hepatocytes contain coarse intracytoplasmic bile-pigment granules with individual-cell necrosis and pigment-laden macrophages. H&E, ×400.

Pancreatic morphological changes

The pancreas showed morphological evidence of biliary reflux and secondary acinar injury. Bile-tinged fluid was identified within the lumen of the main and lobular excretory ducts (Figure 3), and the acini draining into an affected duct showed segmental coagulative necrosis of the acinar epithelium, together with hyaline-droplet and hydropic degeneration of the surviving acinocytes. Around the larger ducts, periductal connective tissue was thickened and, in the more advanced cases, replaced by dense, hyalinised fibrous tissue, producing a pattern of periductal sclerosis (Figure 4). The parenchyma showed marked microvascular congestion, perivascular and periductal lymphohistiocytic infiltration, foci of neutrophilic infiltration with phagocytic activity around necrotic areas, interstitial oedema, and, in the more severe cases, foci of fibrinoid swelling and perivascular hyalinosis (Figure 5). Islets of Langerhans did not show frank necrosis but were reduced in cross-sectional area, with an altered ratio of pale-staining to dark-staining endocrine cells, consistent with diminished secretory activity. In advanced cases, capsular oedema, subcapsular congestion, foci of adipose-tissue invagination between lobules, and intraductal and periepithelial calcification were additionally observed.

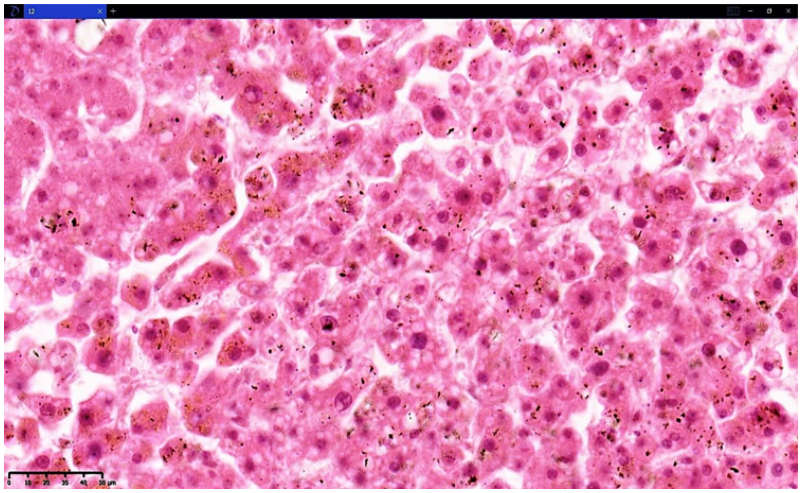

Figure 2. Liver, intrahepatic cholestasis of pregnancy. Diffuse, finely granular cytoplasmic bile pigment with cytoplasmic expansion and hydropic degeneration in zone 2–3 hepatocytes. H&E, ×400.

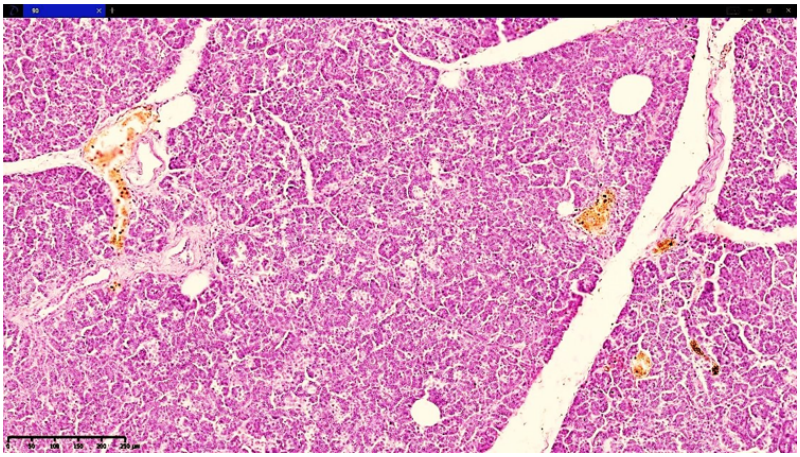

Figure 3. Pancreas, intrahepatic cholestasis of pregnancy. Low-power view of pancreatic lobules with a bile-containing excretory duct (upper left) and mild interlobular changes. H&E, ×100.

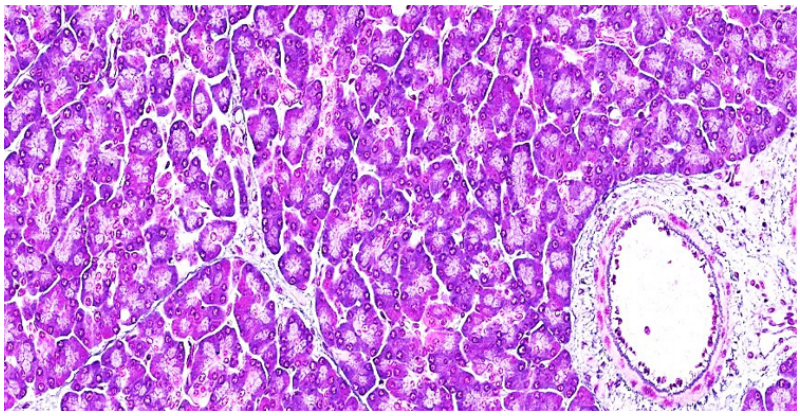

Figure 4. Pancreas, intrahepatic cholestasis of pregnancy. Main excretory duct surrounded by thickened, hyalinised periductal connective tissue (periductal sclerosis), with adjacent acinar atrophy. H&E, ×100.

Quantitative morphometric findings

All twelve morphometric parameters differed significantly between the ICP and control groups (Table 1). Compared with controls, ICP cases showed a smaller mean acinocyte nuclear diameter (5.12±0.28 vs 6.45±0.32 μm; P <0.001) and reduced acinar cytoplasmic area (112.4±5.8 vs 145.8±6.4 μm^2; P <0.001), consistent with cellular atrophy and dystrophy. The mean cross-sectional

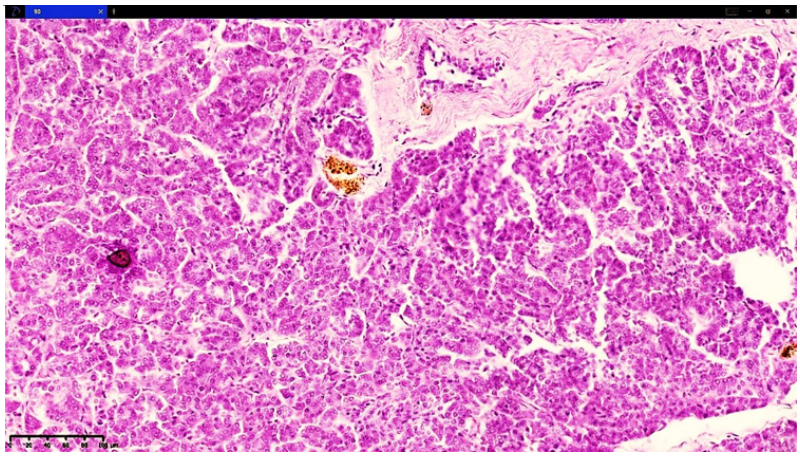

Figure 5. Pancreas, intrahepatic cholestasis of pregnancy. Acinar parenchyma with periductal/perivascular lymphohistiocytic infiltration and scattered pigment deposition. H&E, ×100.

area of the islets of Langerhans was smaller in ICP cases (2680.2±112.9 vs 3205.4±124.6 μm^2; P <0.01). Interstitial and vascular parameters increased markedly: interstitial thickness (38.7±4.2 vs 12.4±1.5 μm), mean capillary/venular diameter (18.5±2.1 vs 7.8±0.9 μm) and the microvascular congestion index (3.9±0.5 vs 1.0±0.2) were all significantly higher in ICP cases (all P <0.001). Degenerative and inflammatory indices were likewise elevated: the proportion of acinocytes with vacuolar/granular dystrophy (46.8±5.1% vs 4.2±0.8%), the number of apoptotic/necrotic cells per field (9.4±1.2 vs 1.1±0.3), periductal inflammatory infiltration density (74.6±8.3 vs 15.2±2.6 units/mm^2), diapedetic haemorrhagic foci (6.8±1.1 vs 0.5±0.2 units/mm^2), connective-tissue proportion (16.3±2.4% vs 5.1±0.7%) and ductal-epithelial desquamation index (28.4±3.7% vs 2.3±0.5%) were all significantly higher in ICP cases than in controls (all P <0.001).

Table 1. Pancreatic morphometric parameters in ICP cases versus controls (mean ± SD).

Morphometric parameter	Control group (n=12)	ICP group (n=28)	P value
Acinocyte nuclear diameter (μm)	6.45 ± 0.32	5.12 ± 0.28	< 0.001
Acinar cell cytoplasmic area (μm^2)	145.8 ± 6.4	112.4 ± 5.8	< 0.001
Mean area of islets of Langerhans (μm^2)	3205.4 ± 124.6	2680.2 ± 112.9	< 0.01
Pancreatic interstitium thickness (μm)	12.4 ± 1.5	38.7 ± 4.2	< 0.001
Mean diameter of capillaries/venules (μm)	7.8 ± 0.9	18.5 ± 2.1	< 0.001
Acinocytes with vacuolar/granular dystrophy (%)	4.2 ± 0.8	46.8 ± 5.1	< 0.001
Apoptotic/necrotic cells per field (n)	1.1 ± 0.3	9.4 ± 1.2	< 0.001
Periductal inflammatory infiltration density (units/mm^2)	15.2 ± 2.6	74.6 ± 8.3	< 0.001
Diapedetic haemorrhagic foci (units/mm^2)	0.5 ± 0.2	6.8 ± 1.1	< 0.001
Connective-tissue proportion (%)	5.1 ± 0.7	16.3 ± 2.4	< 0.001
Ductal-epithelial desquamation index (%)	2.3 ± 0.5	28.4 ± 3.7	< 0.001
Microvascular congestion index	1.0 ± 0.2	3.9 ± 0.5	< 0.001

Relationship with pregnancy parity

Stratification of the combined autopsy series (n=63; 51 ICP and 12 control cases) by parity showed that seven cases occurred in the first pregnancy, 41 in the third pregnancy, 11 in the fourth pregnancy and four in the fifth pregnancy, with the third and fourth pregnancies together accounting

for the large majority of severe ICP-associated pancreatic pathology. When morphological severity was mapped against parity (Table 2), women in their first or second pregnancy showed predominantly vascular changes (capillary dilatation, perivascular oedema, occasional diapedetic haemorrhage) with little or no pancreas-referable clinical expression; women in the third pregnancy showed an intermediate pattern of periductal sclerosis, acinar dystrophy and focal necrosis together with transient or gestational hyperglycaemia; and women in the fourth or later pregnancies showed the most advanced pattern, with massive periductal and perilobular sclerosis (pancreatic fibrosis), angiosclerosis, shrinkage and dystrophy of the islets of Langerhans, and clinical features consistent with a hepato-biliary-pancreatic syndrome with latent exocrine insufficiency.

Table 2. Clinical-morphological grading of pancreatic involvement by pregnancy parity (based on 63 autopsy cases).

Pregnancy parity	**Severity**	**Principal pathomorphological features**	**Clinical expression**
1st pregnancy	Mild / initial	Predominantly vascular changes: capillary dilatation, perivascular oedema, occasional diapedetic haemorrhage.	Usually latent or minimal; few pancreas-referable complaints.
3rd pregnancy	Moderate	Interstitial-pancreatitis pattern; early periductal sclerosis; acinar dystrophy with focal necrosis.	Transient/gestational hyperglycaemia.
4th pregnancy and beyond	Severe	Massive periductal/perilobular sclerosis (pancreatic fibrosis), perivascular angiosclerosis, shrinkage and dystrophy of islets of Langerhans.	Hepato-biliary-pancreatic syndrome; latent exocrine insufficiency; exacerbation of otherwise silent chronic disease.

Discussion:

This autopsy-based study demonstrates that intrahepatic cholestasis of pregnancy is associated with reproducible, quantifiable structural injury to the pancreas that parallels — and, in advanced cases, may outlast — the well-recognised hepatic cholestatic lesion. All twelve morphometric indices distinguished ICP cases from controls with high statistical confidence, and the constellation of segmental acinar necrosis, periductal sclerosis, microvascular congestion and islet shrinkage more closely resembles a chronic, low-grade obstructive-toxic pancreatitis than an incidental post-mortem artefact.

These findings are consistent with, and mechanistically plausible in light of, current understanding of bile acid biology. Once serum and biliary bile acid concentrations exceed physiological thresholds, bile acids act as direct detergents on cell membranes and as signalling ligands for FXR and TGR5, receptors expressed not only in hepatocytes and cholangiocytes but also, functionally, in ductal and acinar pancreatic epithelium, reflecting the shared embryological origin and anatomical continuity of the extrahepatic biliary tree and the main pancreatic duct [6–8]. Activation of TGR5–cAMP–PKA–CREB signalling has been shown to drive epithelial–mesenchymal transition and transforming growth factor-β1-mediated fibrosis in cholangiocytes exposed to retained bile [8], a pathway that could plausibly extend to periductal pancreatic fibroblasts and help explain the periductal sclerosis observed here. Similarly, the bile-acid-induced mitochondrial dysfunction and Bcl-2/Bax-mediated apoptosis documented in ICP placental trophoblasts [9,10] provide a mechanistic template for the acinar-cell necrosis and dystrophy observed in the present series, since both cell types are exposed to comparably elevated systemic bile acid concentrations. A genome-wide association meta-analysis reporting genetic susceptibility loci shared between ICP and acute pancreatitis [11] lends independent, population-level support to a true biological association rather than a chance histological coincidence, and case reports of clinically overt pancreatitis in the setting of severe ICP or acute fatty liver of pregnancy [12,13] indicate that, in a minority of women, this sub-clinical morphological injury may cross the threshold into overt disease.

The relationship between parity and ICP is complex. Larger cohort studies have found that a parity of one or more pregnancies is associated with a reduced risk of developing ICP in a given pregnancy [15]. Our findings do not contradict this: rather, they concern women who had already developed ICP, in whom the severity of pancreatic structural injury increased with successive affected pregnancies, being most advanced in the third and fourth pregnancies. This is compatible with a

cumulative-exposure model, in which repeated episodes of gestational bile acid elevation produce incremental, only partially reversible structural damage to the pancreatic interstitium and ductal system, analogous to the cumulative fibrotic response observed in recurrent biliary obstruction outside pregnancy. Nutritional and metabolic co-factors may compound this effect: ICP is itself associated with reduced gestational weight gain and multiple micronutrient deficiencies [16], and, separately, maternal metabolic stress is known to impair fetal and offspring pancreatic islet development and β-cell mass [20,21], suggesting that the maternal–fetal pancreatic axis as a whole may be particularly vulnerable during cholestatic pregnancies.

From a clinical standpoint, current guidance for ICP centres on serial bile acid measurement, ursodeoxycholic acid therapy and individualised timing of delivery to reduce the risk of stillbirth [2,5]. Our findings suggest that, in women with severe or recurrent ICP — particularly those in their third or later pregnancy — clinicians might reasonably consider screening for subclinical pancreatic involvement (serum amylase/lipase, or careful attention to epigastric symptoms), given that a definable minority of ICP cases in the literature progress to overt pancreatitis [12,13]. Rapid, automated enzymatic bile acid assays now allow same-day quantification of total bile acids [22], which could, in principle, support closer biochemical surveillance in these women without the turnaround delay associated with chromatographic methods.

A methodological strength of this study is the use of digital whole-slide scanning and standardised field-of-view morphometry, an approach increasingly favoured over purely qualitative assessment because it yields reproducible, quantifiable indices amenable to formal statistical comparison [18,19].

This study has several limitations. First, because material was derived exclusively from autopsy cases, the findings necessarily represent the most severe, fatal end of the ICP spectrum and cannot be extrapolated to the much larger population of women with mild, medically managed ICP. Second, the retrospective, single-centre design and modest sample size — particularly the 28-case morphometric subset — limit statistical power and generalisability. Third, no antemortem biochemical or functional pancreatic data (amylase, lipase, faecal elastase) were available for correlation with the morphological findings. Finally, although the control group was free of hepatobiliary or pancreatic disease, it was drawn from women who died of acute myocardial infarction and may not fully represent a metabolically "normal" comparator.

Prospective, multicentre studies combining biochemical pancreatic markers, imaging and, where feasible, biopsy-based morphometry in women with varying ICP severity and parity are warranted to confirm and extend these observations, and to determine whether pancreatic involvement contributes independently to the adverse maternal and perinatal outcomes already attributed to ICP.

Conclusions

Intrahepatic cholestasis of pregnancy should be regarded as a systemic, bile-acid-mediated disorder rather than a condition confined to the hepatobiliary tree. In this autopsy series, severe ICP was consistently accompanied by quantifiable pancreatic injury — acinar dystrophy and necrosis, periductal sclerosis, microvascular congestion and islet shrinkage — that paralleled the well-established hepatic lesion and increased in severity with successive affected pregnancies, particularly the third and fourth. These findings support incorporating pancreatic awareness into the clinical evaluation of women with severe or recurrent ICP and provide a morphological rationale for prospective studies of pancreatic exocrine and endocrine function in this population.

Authors' contribution Conceptualisation, B.L.K.; methodology, B.L.K. and S.R.K.; investigation (autopsy material, histology and morphometry), S.R.K.; formal analysis, S.R.K.; writing—original draft preparation, S.R.K.; writing—review and editing, B.L.K.; supervision, B.L.K. All authors have read and agreed to the published version of the manuscript.

Funding source This research received no external funding.

Ethics approval This study was conducted in accordance with the Declaration of Helsinki and approved by the Scientific Committee (Institutional Ethics Committee) of the Fergana Medical Institute of Public Health (FMIOPH), minutes dated 25 September 2025.

Consent for publication. Patient consent was waived because the study used retrospective, de-identified archival autopsy material collected during routine forensic-pathological

examination; no antemortem clinical intervention or data collection was performed for the purposes of this study.

Data Availability Statement The morphometric datasets generated and analysed during the current study are available from the corresponding author on reasonable request.

Acknowledgments The authors thank the staff of the Republican Scientific and Practical Center of Pathological Anatomy for archival material support.

Conflict of interest The authors declare no conflict of interest.

Abbreviations

ICP	Intrahepatic cholestasis of pregnancy
H&E	Haematoxylin and eosin
SD	Standard deviation
FXR	Farnesoid X receptor
UDCA	Ursodeoxycholic acid

References

[1] Gandhi S, Barsanti-Innes B, Jolicoeur G, Nwokoro IN. Intrahepatic cholestasis of pregnancy. Clin Liver Dis. 2026;30(3):677–699. https://doi.org/10.1016/j.cld.2026.04.009.

[2] Jurk S, Kremer A, Schleussner E. The latest on intrahepatic cholestasis of pregnancy – update 2026. Geburtshilfe Frauenheilkd. 2026;86(6):528–537. https://doi.org/10.1055/a-2845-6610.

[3] Capatina N, Ovadia C. Meta-analyses in cholestatic pregnancy: the outstanding clinical questions. Obstet Med. 2024;17(3):147–151. https://doi.org/10.1177/1753495X241251425.

[4] Niculae LE, Petca A. Intrahepatic cholestasis of pregnancy: neonatal impact through the lens of current evidence. Biomedicines. 2025;13(9):2066. https://doi.org/10.3390/biomedicines13092066.

[5] Kothari S, Afshar Y, Friedman LS, Ahn J. AGA clinical practice update on pregnancy-related gastrointestinal and liver disease: expert review. Gastroenterology. 2024;167(5):1033–1045. https://doi.org/10.1053/j.gastro.2024.06.014.

[6] Zollner G, Trauner M. Mechanisms of cholestasis. Clin Liver Dis. 2008;12(1):1–26.

[7] Yuan S, Zhou S. Mechanistic basis and translational potential of traditional Chinese medicine in the treatment of cholestasis: a narrative review. Hepat Med. 2026;18:609530. https://doi.org/10.2147/HMER.S609530.

[8] Tang D, Yang J, Shi X, Gu X, Zhao L. Activation of the TGR5/cAMP/PKA/CREB axis in cholangiocytes mediates epithelial-mesenchymal transition and fibrosis in hepatolithiasis. Biol Direct. 2026;21(1). https://doi.org/10.1186/s13062-026-00783-7.

[9] Huang X, Liao E, Chen A, Shao Y. Mechanism of mitochondrial dysfunction on placental trophoblastic cells in intrahepatic cholestasis of pregnancy. J Mol Histol. 2025;56(3):140. https://doi.org/10.1007/s10735-025-10427-1.

[10] Xu ZT, Ge LX, Luo L, Ma HY, Xiao H, Ding YB. PIP2 accumulation in the spongiotrophoblast drives trophoblast apoptosis in intrahepatic cholestasis of pregnancy. Mol Reprod Dev. 2026;93(4):e70105. https://doi.org/10.1002/mrd.70105.

[11] Tyrmi JS, Karjalainen J, Venkatesh SS, Benoit-Pilven C, Lemmelä SM, Brunak S, et al. Genome-wide meta-analysis identifies genetic drivers of bile acid metabolism in intrahepatic cholestasis of pregnancy. Nat Commun. 2026;17(1). https://doi.org/10.1038/s41467-026-73122-z.

[12] English N, Rao J. Acute fatty liver of pregnancy with hypoglycaemia, diabetes insipidus and pancreatitis, preceded by intrahepatic cholestasis of pregnancy. BMJ Case Rep. 2015;2015:bcr2015209649. https://doi.org/10.1136/bcr-2015-209649.

[13] Yosief S, Chen W, Wescoe K, Branch MS, Bashir M, Wegermann K. Perplexing severe cholestasis in the postpartum period. ACG Case Rep J. 2026;13(5):e02115. https://doi.org/10.14309/crj.0000000000002115.

[14] Beuers U. Drug insight: mechanisms and sites of action of ursodeoxycholic acid in cholestasis. Nat Clin Pract Gastroenterol Hepatol. 2006;3(6):318–328.

[15] Chen Y, Zhang H, Ning W, Chen Y, Wen C. The impact of intrahepatic cholestasis on pregnancy outcomes: a retrospective cohort study. BMC Gastroenterol. 2023;23(1):16. https://doi.org/10.1186/s12876-023-02652-3.

[16] Keles E, Kaya L, Ogunc YT, Kaya Z, Baydili KN, Kumru P. Impact of maternal nutrition and gestational weight gain on perinatal outcomes in intrahepatic cholestasis of pregnancy. Rev Assoc Med Bras. 2026;72(3):e20251795. https://doi.org/10.1590/1806-9282.20251795.

[17] Öztürk Ö, Çirkin Tekeş G, Şimşek M, Küçükkayıkçı AS, Yakut Yücel K. The evaluation of Xenin-25 levels in intrahepatic cholestasis of pregnancy and comparison with healthy pregnant women. BMC Pregnancy Childbirth. 2026;26(1). https://doi.org/10.1186/s12884-026-09234-7.

[18] Tsuru T, Watanabe T, Kouzu K, Yamagishi Y, Einama T, Yamasaki T, et al. A simple morphometric algorithm based on nuclear atypia features of invasive breast carcinoma: relationship with nuclear grade, Ki-67 level, and hormone receptor status. Breast Cancer. 2026;33(4):905–918. https://doi.org/10.1007/s12282-026-01870-3.

[19] Ono D, Kawai H, Kuwahara H, Yokota T. Refining muscle morphometry through machine learning and spatial analysis. Neuropathol Appl Neurobiol. 2025;51(2):e70012. https://doi.org/10.1111/nan.70012.

[20] Sales DC, Fontes CC, Zanella AP, Martinez C, Souza-Sporkens JC, Vanzela EC, et al. Maternal high-fat diet impairs pancreatic β-cell development and reduces VAMP-2 levels in islets of mouse offspring. J Dev Orig Health Dis. 2026;17:e32. https://doi.org/10.1017/S2040174426100646.

[21] Kumar PU, Ramalaxmi BA, Venkiah K, Sesikeran B. Effect of maternal undernutrition on human foetal pancreas morphology in second trimester of pregnancy. Indian J Med Res. 2013;137(2):302–307.

[22] Kodger J, Nadim H, Choucair I, Sutphin A, Eid T, El-Khoury JM. Rapid diagnosis of intrahepatic cholestasis of pregnancy (ICP): validation of an automated enzymatic total bile acid assay and assessment of ursodeoxycholic acid impact on bile acid profiles in an ICP cohort. J Appl Lab Med. 2026. https://doi.org/10.1093/jalm/jfag099.